Usability of bowtie filter full-fan mode over half-fan mode in cone-beam computed tomography scanning - A prospective study

W.K. Choi¹, W. Park¹, S. Kim²*

¹Department of Radiation Oncology, Samsung Medical Center, Sungkyunkwan University School of Medicine, Seoul, Republic of Korea
²Department of Radiological Science, Gachon University Medical Campus, Incheon, Korea

► *Original article*

ABSTRACT

Background: Using cone-beam computed tomography (CBCT) in radiotherapy, the thorax or pelvis, which are both large areas, can be scanned by rotating the gantry 360° using a half-fan (HF) bowtie filter (BF). The HF mode has a longer scan time than that of the full-fan (FF) mode, thus exposing the patient to an increased imaging dose. **Materials and Methods:** To determine the applicability of FF to anatomically large areas, positioning error values and absorbed dose of organs at risk (OARs) were measured when HF and FF were employed in 22 patients who underwent pelvic intensity-modulated radiation therapy. **Results:** In a clinical experiment applying FFBF scan mode to anatomically large areas of a patient's body during CBCT, the positioning error values were measured for all target areas within the mean ± 3 mm in all three directions. The scanning time in the FF scan mode was reduced by 20 s, while the absorption dose was reduced by 7–52 times in the OARs. **Conclusion:** The appropriate application of FF for treating large-size targets can reduce the CBCT scanning time, which, in turn, would markedly decrease the radiation exposure in patients by reducing random errors during procedures.

INTRODUCTION

Cone-beam computed tomography (CBCT) is used to assess the accuracy of patient positioning before intensity-modulated radiation therapy (IMRT) [1-2]. Furthermore, CBCT has advanced from a tool for verifying three-dimensional (3D) images in image-guided radiation therapy (IGRT) to allowing the adjustment of patient positioning according to the location information for both targets and organs at risk (OAR) provided by CBCT [3-4]. However, the overall treatment duration has increased, given the inclusion of a process for reconstructing the obtained images. Furthermore, CBCT generates more artifacts than those generated by conventional computed tomography (CT). Considering the regular application of CBCT as a tool for setup correction, increased radiation exposure to patients is another limitation, given the increased number of X-ray images, i.e., up to 600–700 within 1 min [5-6].

In current clinical practice, CBCT has been employed for two purposes prior to treatment: 1) to monitor changes in factors governing treatment during IMRT, typically performed up to 20–40 times, followed by the prompt application of adaptive radiation therapy, and 2) to correct both patient positioning errors and existing images for treatment-planning CT during the pre-review process of CBCT images before each treatment.

An aluminum bowtie filter (BF) is used to obtain CBCT images for positioning error corrections, since BF can reduce the skin dose and improve the image quality [7]. BFs are divided into two types based on the anatomical size of the human body when CBCT scanning is implemented in radiation therapy. Scan images for small areas, such as the head and neck, can be obtained using a full-fan (FF) with a gantry rotation angle of 200°, whereas images for larger areas, such as the thorax and pelvis, can be obtained using a half-fan (HF) with a gantry rotation angle of 360°. HF can generate superior images owing to the acquisition of large amounts of projection data. However, HF increases the scanning time, consequently increasing the imaging dose exposure of patients [8-9].

In recent years, the Halcyon 3.0 linear accelerator (Varian Medical Systems, Palo Alto, CA) comprises a kV (kilo voltage) imaging system orthogonal to the treatment beam and inline mega-voltage (MV) imaging for daily CBCT. An additional imaging dose is required owing to the geometry of the Halcyon. Li *et al.* have observed normal tissue doses in an anthropomorphic phantom from MV imaging [10], whereas Malajovich et al. have documented doses ranging from 8.02 mGy (in orthogonal planar MV imaging) up to 84.48 mGy (in MV-CBCT mode) for a single fraction [11].

Accordingly, studies have explored the possibility

of minimizing the imaging dose received by patients [12-13], most of which were performed using a Catphan 504 phantom (The Phantom Laboratory, Salem, NY) and a solid water phantom (manufactured by Gammex-RMI) for CBCT quality assurance (QA). However, its application among patients remains limited, given the small size of the QA phantom and lack of anatomical information. Therefore, alternative approaches are urgently required to reduce the imaging dose.

We had previously examined the potential of FF to target organs that are anatomically large areas of a patient's body, revealing promising results using a human phantom and confirming the applicability of FF in pelvic IMRT, which is typically performed using HF in clinical settings [14]. The effective dose for the FF scan of the head region was 0.18 mSv, whereas that for the HF scan of the pelvic region was 0.51 mSv [15]. The scan times between HF and FF scans (60 s and 40 s, respectively) differed by approximately 20 s. Hence, in the present study, we investigated the correction values for errors calculated by applying HF and FF to actual patients. Moreover, we examined the applicability of FF to anatomically large areas of the patient's body by comparing the absorption dose for each organ based on the CBCT images obtained using the HF and FF scan modes.

MATERIALS AND METHODS

Patient cohort

This study was approved by the Institutional Review Board (IRB No. 2018-07-110) of Samsung Medical Center, Seoul, South Korea. All patients provided written informed consent and received a comprehensive explanation of the purpose of the study. Among the 23 patients who received pelvic IMRT at Hospital A, located in Seoul, from December 2018 to July 2019, 22 participated in the present study, except for one patient who had uterine sarcoma, with difficulties in identifying the target location and size when FF was applied. The average age of the patients was 61 years (range, 36–82 years) (table 1).

Table 1. Patient characteristics.

Site	Patient number (n = 22)	Male (n = 7)	Female (n = 15)	Age in years (mean)
Cervical cancer	8		8	58.1
Bladder cancer	4	4		69
Rectal cancer	3	2	1	51
Uterine sarcoma	2		2	56
Vulvar cancer	2		2	67.5
Inguinal	1		1	81
Genital	1	1		73
Coccyx	1		1	59

Image acquisition

For treatment planning, Discovery CT590 RT (GE Healthcare, USA) was performed according to the manufacturer's protocol (field of view, 40 cm; matrix, 512×512; slice thickness, 2.5 mm). Images were then forwarded to the radiation therapy planning software (Pinnacle3, Philips, USA) installed at Hospital A. The treating physician outlined the treatment-planning target volume on obtained images, and a dosimetrist drew the OAR outline. The IMRT plan was established according to the protocol at Hospital A. After verification by both the treating physician and the oncologist, data were forwarded to the treatment room. The Novalis Tx system (Novalis Tx TM system, Varian, USA), a linear accelerator, was used to obtain the CBCT images.

Six CBCT modes were used in the treatment room, namely low-dose head, standard-dose head, high-quality head, pelvis, pelvic spotlight, and low-dose thorax. Currently, for pelvic IMRT in clinics, the pelvis mode (125 kV, 80 mA, 13 ms, 360° gantry rotation), an HF mode (On Board Imager [Varian Medical Systems, Palo Alto, CA]; Blade: x1=6.8 cm, x2=23.5 cm and y1=y2=10.3 cm), is used to obtain high-resolution images, given its ability to scan large areas and acquire a considerable amount of projection data. However, in the present study, images were obtained by applying the standard-dose head mode (100 kV, 20 mA, 20 ms, 200° gantry rotation), an FF method used in existing head and neck IMRT, and the Felvis mode-an HF method-to the same patient every other day. The parameters set for the CBCT scan were the same as those used for treatment-planning CT images, with a slice thickness of 2.5 mm and a reconstruction volume of 512×512.

Comparison of positioning error values

To correct patient positioning errors, 3D/3D matching was performed between CBCT and treatment-planning CT images by referencing outlines drawn along the anatomical structure of bones on the planning CT images [16-17]. An experienced radiologist reviewed the images and performed manual corrections for the target (marked in orange in figure 1) and nearby OAR (marked in red in figure 1).

To correct errors using the isocenter of each patient as a reference point, shift values were placed within ±3 of the margin of error for all three directions, including the x-axis (lateromedial view), y-axis (craniocaudal view), and z-axis (anterior-posterior view), when performing pelvis IMRT. Additionally, 3D vector values, that is, indices of the displacement results from the reference point, were calculated using equation 1 [18].

$$3D\ Vector = \sqrt{X^2 + Y^2 + Z^2} \qquad (1)$$

Subsequently, shift values were forwarded to the linear accelerator and used to move the couch automatically to correct positioning errors. To compare HF and FF scan modes, all patients were scanned between the two modes every alternate day.
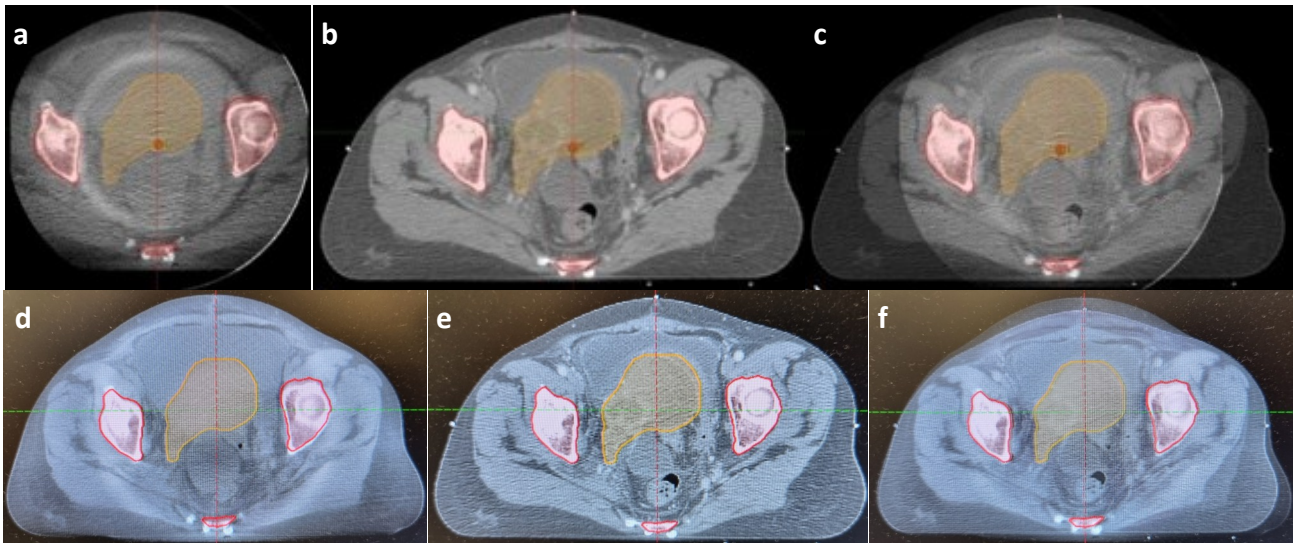
Figure 1. Image matching process **(a)** FF CBCT, (b) Planning CT, **(c)** overlap image of FF CBCT and planning CT, **(d)** HF CBCT, **(e)** Planning CT, **(f)** overlap image of HF CBCT and planning CT. Target (marked in orange color), nearby OAR (marked in red color). CBCT, cone-beam computed tomography; CT, computed tomography; FF, full-fan; OAR, organs at risk.

Dose measurements

Considering CBCT for pelvic IMRT, doses absorbed by the OAR were measured in HF and FF modes. In total, five glass dosimeters (Dose Ace GD-302M, Asahi Techno Glass Corporation Shizuoka, Japan) were inserted into the human phantom (RANDO®, Alderson Research Laboratories Inc., Stanford, CT, USA): the bladder, rectal, small bowel, and left and right side of the femoral head, one each. The doses were measured using a dosimetry system (Dose Ace FGD-1000; Asahi Techno Glass Corporation, Shizuoka, Japan).

Based on the above-described conditions, the positioning was determined using the imaginary isocenter (pelvis median line and mid-depth) as a reference, and the CBCT scan was performed by alternating the two scan modes, i.e., HF and FF. To monitor the change in absorption dose for each organ according to changes in the isocenter point, the absorbed dose was measured by moving the isocenter point by ± 5 cm in the direction of the z-axis (anterior-posterior). The conditions used for dose measurement were based on a reference guidebook [19] (acquisition angle 200° at FF, 100 kV, 20 mA, 20 ms at FF, acquisition angle 360° at HF, 125 kV, 80 mA, 13 ms), and all measurements were repeated five times.

Statistical analysis

Data were analyzed using the Statistical Package for the Social Sciences (SPSS version 22.0; IBM, New York, USA). One-way analysis of variance (ANOVA) and two-way ANOVA were performed to compare patient positioning errors between HF and FF images (i.e., the positioning errors between the CBCT HF and planning CT images were compared with those between the CBCT FF and planning CT images). The BF method (HF and FF) and axial direction (x-, y-, and z-axes) were used as independent variables in the two-way ANOVA. p-values <0.05 were deemed significant.

RESULTS

Patient positioning error values

Among the 22 participants, 352 CBCT images (HF and FF, 176 each) were superimposed on the treatment-planning CT images, and patient positioning error values were compared. Selecting the HF mode, the average for each axis was as follows: x-axis, 0.12 ± 0.11 cm; y-axis, 0.29 ± 0.33 cm; and z-axis, 0.25 ± 0.17 cm. Selecting the FF mode, the average for each axis was as follows: x-axis, 0.13 ± 0.14 cm; y-axis, 0.29 ± 0.27 cm; and z-axis, 0.27 ± 0.18 cm. The 3D vector values representing the errors induced by 3D parallel displacement in 3D space were 0.45 ± 0.24 cm and 0.49 ± 0.25 cm for HF and FF scans, respectively. Considering cervical, bladder, and rectal cancers, the difference in patient positioning error values at HF and FF scan modes was less than ± 0.1 cm in all directions, and the inguinal area showed error values of 0.29 and 0.06 cm for 3D vector and y-axis, respectively (table 2).

One-way ANOVA of the error values collected from the x-, y-, and z-axes and the 3D vector from the CBCT images mentioned above revealed no statistically significant differences between the HF and FF scan modes: x-axis, F=0.871, p=0.351; y-axis, F=0.015, p=0.902; z-axis, F=1.091, p=0.300; and 3D Vector, F=0.633, p=0.427 (table 3).

As shown in Table 4, two-way ANOVA revealed no statistically significant difference in error values between the HF and FF scan modes when using the BF method (HF and FF) and axial direction (x-, y-, and z-axes) as independent variables (F=1.968, p=0.160).

Despite a significant difference among the three axes (F=67.5, p<0.001), there was no significant difference in the interaction effect between the two variables (F=0.037, p=0.963). Accordingly, no separate post-analysis was performed (table 4).

Dose measurements

The absorption dose received by the OAR during CBCT in the HF mode was measured five times repeatedly, with the isocenter set to the pelvic median line with middle depth. The doses received by each organ were as follows: bladder, 12.2±0.04 cGy; rectum, 8.59±0.01 cGy; small bowel, 13.4±0.06 cGy; left femoral head, 8.49±0.00 cGy; and right femoral head, 7.57±0.01 cGy.

In the FF mode, the doses received by each organ were as follows: bladder, 0.36±0.00 cGy; rectum, 1.17±0.00 cGy; small bowel, 0.26±0.00 cGy; left femur, 0.74±0.00 cGy; and right femur, 0.35±0.00 cGy. The FF-to-HF dose ratio ranged from a minimum of 7.34 times (rectum) to a maximum of 51.69 times (small bowel). Subsequently, the isocenter set to the pelvic median line with a middle depth was placed +5 cm along the z-axis (anterior-posterior). In the HF mode, the dose ranged from 7.45±0.01 to 15.17±0.04 cGy. In the FF mode, the dose ranged from 0.36±0.00 cGy to 0.91±0.00 cGy. The maximum FF-to-HF dose ratio was 42.14 times. When the isocenter set to pelvic median line with middle depth was placed -5 cm along the z-axis (anterior-posterior), the maximal FF-to-HF dose ratio was 52.00 times (table 5).

Table 2. Comparison of localization accuracy between half-fan and full-fan modes (patients, n = 176).

Site	HF				FF			
	LR (x-axis)	SI (y-axis)	AP (z-axis)	3D Vector	LR (x-axis)	SI (y-axis)	AP (z-axis)	3D Vector
Cervical cancer	0.19	0.19	0.34	0.48	0.28	0.18	0.38	0.58
	0.13	0.29	0.33	0.49	0.13	0.32	0.34	0.51
	0.17	0.17	0.07	0.26	0.45	0.20	0.10	0.51
	0.20	0.30	0.18	0.42	0.11	0.34	0.13	0.42
	0.23	0.38	0.05	0.47	0.53	0.47	0.07	0.72
	0.18	0.08	0.10	0.23	0.30	0.20	0.20	0.45
	0.09	0.24	0.34	0.46	0.09	0.21	0.34	0.43
	0.03	0.13	0.17	0.22	0.05	0.15	0.10	0.20
Mean	0.15	0.22	0.20	0.38	0.24	0.26	0.21	0.48
Bladder cancer	0.12	0.14	0.17	0.28	0.07	0.19	0.22	0.32
	0.08	0.35	0.13	0.40	0.12	0.44	0.10	0.48
	0.15	0.08	0.12	0.24	0.13	0.05	0.18	0.28
	0.11	0.10	0.16	0.25	0.11	0.16	0.08	0.25
Mean	0.12	0.17	0.14	0.29	0.11	0.21	0.15	0.33
Rectal cancer	0.03	0.10	0.07	0.13	0.00	0.10	0.05	0.12
	0.11	0.18	0.85	0.91	0.08	0.24	0.73	0.83
	0.07	0.39	0.12	0.44	0.12	0.41	0.15	0.47
Mean	0.07	0.22	0.35	0.49	0.07	0.25	0.31	0.47
Uterine sarcoma	0.07	0.23	0.00	0.26	0.10	0.50	0.05	0.52
	0.03	0.33	0.05	0.34	0.10	0.57	0.13	0.60
Mean	0.05	0.28	0.03	0.30	0.10	0.53	0.09	0.56
Vulvar cancer	0.09	0.39	0.21	0.48	0.05	0.39	0.29	0.53
	0.08	0.26	0.42	0.54	0.10	0.25	0.62	0.72
Mean	0.08	0.33	0.32	0.51	0.08	0.32	0.45	0.62
Inguinal	0.00	0.14	0.50	0.52	0.28	0.20	0.70	0.82
Genital	0.05	0.14	0.20	0.30	0.09	0.13	0.30	0.37
Coccyx	0.13	0.09	0.16	0.27	0.16	0.08	0.33	0.40
Mean ± SD	0.12 ± 0.11	0.28 ± 0.26	0.25 ± 0.17	0.45 ± 0.24	0.13 ± 0.14	0.29 ± 0.27	0.27 ± 0.18	0.49 ± 0.25

HF, half-fan; FF, full-fan; LR, left-right; SI, superior-inferior; AP, anterior-posterior; SD, standard deviation

Table 3. One-way analysis of variance for each direction (patients).

	Sum of squares	d.f.	F	p
LR (x-axis)	0.014	1	0.871	0.351
SI (y-axis)	0.001	1	0.015	0.902
AP (z-axis)	0.035	1	1.091	0.300
3D Vector	0.049	1	0.633	0.427

LR, left-right; SI, superior-inferior; AP, anterior-posterior.

Table 4. Two-way analysis of variance on the bowtie filter × axis (patients).

Category		Sum of squares	d.f.	F	p
Main effect	BF	0.078	1	1.968	0.160
	x-, y-, z-axis	5.378	2	67.5	0.000
Interaction effect	BF × x-, y-, z-axis	0.003	2	0.037	0.963
Error		41.831	1,050		

BF, bowtie filter.

Table 5. Average absorbed dose in the OAR (mean ± SD), units: cGy.

		Bladder	Rectal	Small bowel	Left femoral head	Right femoral head
Isocenter	HF	12.22 ± 0.04	8.59 ± 0.01	13.44 ± 0.06	8.49 ± 0.00	7.57 ± 0.01
	FF	0.36 ± 0.00	1.17 ± 0.00	0.26 ± 0.00	0.74 ± 0.00	0.35 ± 0.00
	HF/FF	33.90	7.34	51.69	11.47	21.62
Isocenter +5 cm	HF	13.42 ± 0.04	7.68 ± 0.00	15.17 ± 0.04	8.79 ± 0.00	7.45 ± 0.01
	FF	0.39 ± 0.00	0.81 ± 0.00	0.36 ± 0.00	0.91 ± 0.00	0.64 ± 0.00
	HF/FF	34.41	9.48	42.14	9.65	11.64
Isocenter -5 cm	HF	9.78 ± 0.00	7.83 ± 0.01	9.36 ± 0.01	7.25 ± 0.01	6.93 ± 0.01
	FF	0.24 ± 0.00	1.11 ± 0.00	0.18 ± 0.00	0.34 ± 0.00	0.27 ± 0.00
	HF/FF	40.75	7.05	52.00	21.32	25.67

OAR, organs at risk; SD, standard deviation; HF, half-fan; FF, full-fan

DISCUSSION

Similar to IMRT, a highly specialized treatment, IGRT is implemented daily after verifying the error correction and the accuracy of patient positioning. Although minimal radiation was employed during the verification process to determine the best position for patients, the cumulative effect of repeated exposure can cause serious health issues.

The present study aimed to reduce the CBCT scan time when conducted daily to confirm patient positioning, as well as to establish the amount of radiation exposure to patients. Accordingly, we evaluated the possible use of FFBF as an alternative to HFBF, which is typically employed to scan anatomically large areas of a patient's body.

According to the scan modes, the patient positioning error values for HF were a minimum value of 0.12 cm (x-axis) and a maximum value of 0.45 cm (3D vector); for FF, the minimum value was 0.13 cm (x-axis), and the maximum value was 0.49 cm (3D vector). As described previously, both scan modes yielded positive results. Compared with the HF scan mode for anatomically large areas, the FF mode did not induce any image distortion or deformation, whereas the scan range moved away from the rotation center axis or around the isocenter. Furthermore, the compatibility of FF to HF was supported by the fact that similar to the phantom experiment results [14], patient positioning error values were within the error range, a mean ± 3 mm, in all three directions, i.e., x-, y-, and z-axes, when a radiologist double-checked images and made secondary corrections after computer-aided automatching using bone images within regions of interest. Furthermore, the difference in patient positioning error values between the HF and FF modes for targets, such as cervical, bladder, rectal cancers, and genital area, was less than ± 0.1 cm in all three directions, thereby indicating that positioning errors did not substantially impact the FF scan mode even when applied to anatomically large areas. However, differences in positioning error values for targets such as the inguinal area and uterine sarcoma between HF and FF were larger than those for the targets mentioned above, ranging from 0.06~0.29 cm.

Several studies have attempted to reduce radiation exposure to patients, such as those by Sykes *et al.* [20], Ding *et al.* [21], and Alvarado *et al.* [22], where the authors reduced the number of image acquisitions, adjusted the start/stop angles of the imaging source, reduced the scan length, and used low-dose (or reduced mAs) protocols instead of standard high-dose protocols. Considering previous reports [9, 15,18], a four-fold difference in the absorption dose was documented between the head and neck area scanned using the FFBF and the pelvic areas scanned using the HFBF. However, reports regarding the application of FFBF in the pelvic area are lacking. To our knowledge, the current study is the first to explore the potential of FFBF in the pelvic region. When measuring the absorption dose at the OAR, we noted a slight difference between FFBF and HFBF modes depending on the isocenter location. However, the difference for each target was distinct from that of OAR: 33.9-40.75 times in the bladder, 7.05-9.48 times in the rectum, 42.14-52 times in the small bowel, and 9.65-25.67 times in the femur. Considering the scan time between HF and FF, the duration of the FF scan mode was 40 s, while that of the HF mode was 60 s; hence, the 20-s reduction in scanning time could help reduce patient exposure to radiation.

Nevertheless, the limitations of the FF mode when scanning large target areas must be addressed. The size of the reconstructed FF images was smaller than that of the HF images owing to the prefixed size of the image area when the FF was applied. The resolution of scan images obtained by FF was low, given the acquisition of minimal projection data. Moreover, beam hardening increased artifacts when the FF scan mode was employed. No studies have reported on solid solutions that can reduce artifacts attributed to the beam-hardening effect [23]. In a preliminary human phantom experiment [14], a beam-hardening effect was observed when applying an FF, with beam diameters and thicknesses of 15 and 0.5 cm, respectively. Considering the experiment performed in patients, one participant was excluded owing to beam hardening-induced artifacts when applying FF, which interfered with the identification of the target location and size. Despite the limitations associated with the use of FF for anatomically large areas, we confirmed the applicability of FF over HF for large areas of the patient's body.

In the future, with additional in-depth research on diseases and potentially positive results of FF application, patients could experience the advantages of shortened scanning time and reduced radiation exposure.

CONCLUSION

We applied the FFBF scan mode to anatomically large areas of the patient's body at CBCT and measured displacement values using positioning error values within the mean ± 3 mm for all target areas in all three directions. The FF scan mode reduced the scanning time by 20 s and the absorption dose by 7–52 times at OARs. In conclusion, the appropriate application of FF for treating large-sized targets could reduce the CBCT scanning time, which, in turn, would markedly reduce radiation exposure in patients by decreasing random errors that may occur during the procedure.

Ethical considerations: All subjects provided informed consent before participating in the study,

which was approved by the Institutional Review Board (IRB No. 2018-07-110) of the Samsung Medical Center (Seoul, South Korea).

Funding: None

Conflicts of interest: The authors declare no conflicts of interest.

Author contributions: Conceptualization and methodology, W. Choi, W. Park, and S. Kim; data collection, analysis, and interpretation of results, W. Choi and W. Park; writing-original draft preparation, W. Choi; writing review and editing, W. Choi, W. Park, and S. Kim. All authors have read and agreed to the published version of the manuscript.

REFERENCES

1. Won YJ, Kim JW, Kim JH (2017) Dose comparison using deformed image registration method on breast cancer radiotherapy. *J Radiological Science and Technology, 40(1): 57-62*.
2. Zhang J, Bao ZR, Huang XT, *et al.* (2019) Methods to evaluate the performance of kilovoltage cone-beam computed tomography in three-dimensional reconstruction space. *Int J Radiat Res, 17(2): 189-202*.
3. Jaffray DA and Siewerdsen JH (2000) Cone-beam computed tomography with a flat-panel imager: initial performance characterization. *Med Phys, 27(6): 1311-23*.
4. Hansen EK, Bucci MK, Quivey JM, *et al.* (2006) Repeat CT imaging and replanning during the course of IMRT for head-and-neck cancer. *Int J Radiat Oncol Biol Phys, 64(2): 355-62*.
5. Islam MK, Purdie TG, Norrlinger BD, *et al.* (2006) Patient dose from kilovoltage cone beam computed tomography imaging in radiation therapy. *Med Phys, 33(6):1573-82*.
6. Kim JH and Bae SH (2017) The effect of patient positioning system on the prescription dose in radiation therapy. *J Radiological Science and Technology, 40(4): 613-20*.
7. Siewerdsen JH and Jaffray DA (2001) Cone-beam computed tomography with a flat-panel imager: magnitude and effects of X-ray scatter. *Med Phys, 28(2): 220-31*.
8. Kumar AS, Singh RR, Sharma SD, *et al.* (2016) Radiation dose measurements during kilovoltage-cone beam computed tomography imaging in radiotherapy. *J Cancer Res Ther, 12(2): 858-63*.
9. Kim S, Sua Y, Yin F, *et al.* (2010) Kilovoltage cone-beam CT: comparative dose and image quality evaluations in partial and full-angle scan protocols. *Med Phys, 37(7): 3648-59*.
10. Li Y, Netherton T, Nitsch PL, *et al.* (2018) Normal tissue doses from MV image-guided radiation therapy (IGRT) using orthogonal MV and MV-CBCT. *J Appl Clin Med Phys, 19(3): 52-7*.
11. Malajovich I, Teo BK, Petroccia H, *et al.* (2019) Characterization of the megavoltage cone-beam computed tomography (MV-CBCT) system on Halcyon™ for IGRT: image quality benchmark, clinical performance, and organ doses. *Front Oncol, 9: 496*.
12. Seet KY, Barghi A, Yartsev S, Dyk JV (2009) The effects of field-of-view and patient size on CT numbers from cone-beam computed tomography. *Phys Med Biol, 54(20): 6251-62*.
13. Kim S and Alaei P (2016) Implementation of full/half bowtie filter models in a commercial treatment planning system for kilovoltage cone-beam CT dose estimations. *J Appl Clin Med Phys, 17(2): 153-64*.
14. Choi W, Park W, Kim S (2021) Usability assessment of cone-beam computed tomography with a full-fan mode bowtie filter compared with that with a half-fan mode bowtie filter. *Int J Radiat Res, 19(1): 231-37*.
15. Cheng HC, Wu VW, Liu ES, Kwong DL (2011) Evaluation of radiation dose and image quality for the Varian cone beam computed tomography system. *Int J Radiat Oncol Biol Phys, 80(1): 291-300*.
16. Hyde D, Lochray F, Korol R, *et al.* (2012) Spine stereotactic body radiotherapy utilizing cone-beam CT image-guidance with a robotic couch: intrafraction motion analysis accounting for all six degrees of freedom. *Int J Radiat Oncol Biol Phys, 82(3): e555-62*.
17. Scarfe WC and Farman AG (2008) What is cone-beam CT and how does it work? *Dent Clin North Am, 52(4): 707-30*.
18. Lin CG, Xu SK, Yao WY, *et al.* (2017) Comparison of setup accuracy among three common immobilization systems for intensity-modulated radiotherapy of nasopharyngeal carcinoma patients. *J Med Radiat Sci, 64(2): 106-13*.
19. Varian Medical Systems Inc. The reference guide provided information and procedures for using the onboard imager application, version 1.4. 2007.
20. Sykes JR, Amer A, Czajka J, Moore C (2005) A feasibility study for image-guided radiotherapy using low-dose, high-speed, cone-beam X-ray volumetric imaging. *Radiother Oncol, 77(1): 45-52*.
21. Ding GX, Munro P, Pawlowski P, *et al.* (2010) Reducing radiation exposure to patients from kV-CBCT imaging. *Radiother Oncol, 97 (3): 585-92*.
22. Alvarado R, Booth JT, Bromley RM, Gustafsson HB (2013) An investigation of image guidance dose for breast radiotherapy. *J Appl Clin Med Phys, 14(3): 25-38*.
23. Niu T and Zhu L (2011) Scatter correction for full-fan volumetric CT using a stationary beam blocker in a single full scan. *Med Phys, 38 (11): 6027-38*.